

1 **2015 Indonesian fire activity and smoke pollution show persistent non-linear**
2 **sensitivity to El Niño-induced drought**

3
4 Robert D. Field^{1,2}, Guido R. van der Werf³, Thierry Fanin³, Eric Fetzer⁴, Ryan Fuller⁴,
5 Hiren Jethva^{5,6}, Robert Levy⁵, Nathaniel Livesey⁴, Ming Luo⁴, Omar Torres⁵, Helen M.
6 Worden⁷

- 7
8
9 1. NASA Goddard Institute for Space Studies
10 2880 Broadway, New York, NY, USA, 10025
11
12 2. Dept. of Applied Physics and Applied Mathematics, Columbia University
13 2880 Broadway, New York, NY, USA, 10025
14
15 3. Faculty of Earth and Life Sciences, Vrije Universiteit Amsterdam
16 De Boelelaan 1085, Amsterdam, Netherlands, 1081HV
17
18 4. Jet Propulsion Laboratory/California Institute of Technology
19 4800 Oak Grove Drive, Pasadena, CA, USA, 91109
20
21 5. NASA Goddard Space Flight Center
22 Mail Code 614 Greenbelt, MD, USA, 20771
23
24 6. Universities Space Research Association, Columbia, MD, USA
25 Mail Code 614 Greenbelt, MD, USA, 20771
26
27 7. National Center for Atmospheric Research
28 3450 Mitchell Lane, Boulder CO, USA, 80301

29 Corresponding author:

30 Robert Field (robert.field@columbia.edu)

31 NASA Goddard Institute for Space Studies

32 2880 Broadway, New York, NY, 10025

33 Tel: (212) 678 5600

34
35 Keywords: Indonesia, fire, biomass burning, atmospheric pollution, drought, El Niño
36

37 **Significance**

38 The 2015 fire season in Indonesia was the most severe observed by the NASA Earth
39 Observing System satellites that go back to the early 2000s in terms of fire activity
40 and pollution. Our estimates show that the 2015 CO₂-equivalent biomass burning
41 emissions for all of Indonesia were in between the 2013 annual fossil fuel CO₂
42 emissions of Japan and India. Longer-term records of airport visibility in Sumatra
43 and Kalimantan show that 2015 ranked among the worst episodes on record.
44 Analysis of yearly dry season rainfall shows that, due to the continued use of fire to
45 clear and prepare land on degraded peat, the Indonesian fire environment continues
46 to have non-linear sensitivity to dry conditions, and this sensitivity appears to have
47 increased over Kalimantan.

48 **Abstract**

49 The 2015 fire season and related smoke pollution in Indonesia was more severe
50 than the major 2006 episode, making it the most severe season observed by the
51 NASA Earth Observing System satellites that go back to the early 2000s, namely
52 active fire detections from the Terra and Aqua Moderate Resolution Imaging
53 Spectroradiometers (MODIS), MODIS aerosol optical depth, Terra Measurement of
54 Pollution in the Troposphere (MOPITT) carbon monoxide (CO), Aqua Atmospheric
55 Infrared Sounder (AIRS) CO, Aura Ozone Monitoring Instrument (OMI) aerosol
56 index, and Aura Microwave Limb Sounder (MLS) CO. The MLS CO in the upper
57 troposphere showed a plume of pollution stretching from East Africa to the western
58 Pacific Ocean that persisted for two months. Longer-term records of airport
59 visibility in Sumatra and Kalimantan show that 2015 ranked after 1997 and
60 alongside 1991 and 1994 as among the worst episodes on record. Analysis of yearly
61 dry season rainfall from the Tropical Rainfall Measurement Mission (TRMM) and
62 rain gauges shows that, due to the continued use of fire to clear and prepare land on
63 degraded peat, the Indonesian fire environment continues to have non-linear
64 sensitivity to dry conditions during prolonged periods with less than 4mm/day of
65 precipitation, and this sensitivity appears to have increased over Kalimantan.
66 Without significant reforms in land use and the adoption of early warning triggers
67 tied to precipitation forecasts, these intense fire episodes will re-occur during future
68 droughts, usually associated with El Niño events. \body

69 **1. Introduction**

70 The 2015 fire season in Indonesia began in July in Sumatra and a month later in
71 Kalimantan, and was mostly confined to the part of the country in the Southern
72 hemisphere. By September, much of Sumatra and Kalimantan were blanketed in
73 thick smoke that lasted through October, with the haze extending to Singapore,
74 Malaysia and Thailand. Millions of people were exposed to hazardously poor air
75 quality for 2 months (1).

76

77 Figure 1 shows the monthly Moderate Resolution Imaging Spectroradiometer
78 (MODIS) active fire detections (described in the next section) between August and
79 November 2015. This period comprised the bulk of the fire season, with 85% of
80 total annual fire detections. September and October were the months with the
81 highest number of active fire detections (68% of total). Most fires burned in the
82 lowlands of southern Sumatra and Kalimantan, often in areas underlain by peat
83 deposits. The locations of the fires and the progression of the fire season resembled
84 2006, but there were more fires in 2015 in the main fire-affected provinces except
85 for western Kalimantan. The key difference with other years is in the amount of fire
86 activity.

87

88 The fire and haze in 2015 was a repeat of events that have occurred periodically in
89 Kalimantan since the 1980s (2-6) and in Sumatra since at least the 1960s (7). From
90 those studies, 1982/83, 1987, 1991, 1994, 1997, and 2006 can be considered
91 'severe' fire years over Sumatra and Kalimantan, relative to years where little or
92 moderate fire occurs because it is too wet during the dry season for sustained
93 burning. Fires are set to clear logging waste, agricultural waste, and, in order to
94 maintain or secure land-tenure, regrowth (8, 9). The fires often occur on drained
95 and degraded peat lands (10). During abnormally dry years typically associated
96 with El Niño conditions, the peat becomes dry enough to burn (11). Fires on the
97 surface can escape underground, where, because they are so difficult to extinguish
98 and have a large source of fuel, they burn continuously until the return of the
99 monsoon rains (12).

100

101 It is widely accepted that the worst event on record was in 1997, with the total CO₂
102 emissions equivalent to between 13-40% of mean annual global fossil fuel
103 emissions at the time (11). The last major event occurred in 2006 over southern
104 Sumatra and south-central Kalimantan, under a combination of moderate El Niño
105 and positive Indian Ocean Dipole conditions (12). The 2006 burning episode
106 registered uniquely in satellite measurements sensitive to pollution in the mid-
107 troposphere (13-15). In terms of extent and duration, retrieved CO in the upper
108 troposphere in 2006 was the highest during the 2004-2011 observation record
109 across the whole of the tropics (16). There have been brief episodes under isolated
110 dry conditions that produced locally high pollution levels, for example in the central
111 Sumatran province of Riau in 2013 (10), but in general fire activity and pollution
112 levels have not approached those of 2006 in the intervening years.

113

114 To quantify the magnitude of 2015 compared to past events and understand the
115 drought conditions under which they occurred, we analyzed data from the NASA
116 Earth Observing System (EOS) period, namely MODIS active fire detections, five
117 different satellite measurements of tropospheric pollution, airport visibility records
118 as a longer-term proxy, and precipitation estimates from satellites and rain gauges.
119 We make the case that the 2015 Indonesian fire season was the most severe season
120 since the NASA's Earth Observing satellite system began observations in the early
121 2000s, and, by examining visibility data prior to the EOS period, that 2015 ranked

122 after 1997 and alongside 1991 and 1994 as among the worst Indonesian fire events
123 on record.

124 **2. Data**

125 During the EOS period, we used mid-tropospheric CO data from the Terra
126 Measurement of Pollution in the Troposphere (MOPITT) (17), and Aqua
127 Atmospheric Infrared Sounder (AIRS) instruments (18), and upper-tropospheric CO
128 data from the Aura Microwave Limb Sounder (MLS) (19). Aerosols were
129 characterized using MODIS aerosol optical depth (AOD) over ocean (20) and land
130 (21), and the Aura Ozone Monitoring Instrument (OMI) aerosol index (AI) (22). Fire
131 activity was characterized by Terra and Aqua MODIS active fire detections (23).
132 Details of these data are provided as supplementary information.

133

134 At the surface, airport visibility is a useful indicator of severe fire emissions in
135 Indonesia (7, 24-26) because of high emissions per unit area burned and poor
136 ventilation due to typically gentle surface winds. Visibility records were obtained for
137 World Meteorological Organization (WMO)-level surface stations located at three
138 airports in each of southern Sumatra (Rengat, Jambi, and Palembang) and south-
139 central Kalimantan (Pangkalan Bun, Palangkaraya, Muaratewe) from the NOAA
140 Integrated Surface Database for 1990-2015. We computed the total extinction
141 coefficient (B_{ext}) from the visibility using the empirical Koschmieder relationship,
142 $B_{\text{ext}} = 1.9/v$, where v is the visibility in km (7). For the sake of computation, reports
143 of zero visibility during the worst of the haze were replaced with 0.05km, the next
144 lowest reported value.

145

146 Precipitation estimates for 2000-2015 were obtained from the Tropical Rainfall
147 Measurement Mission (TRMM) (27) 3B42RT product, which is produced using a
148 consistent retrieval, but lacks radar data assimilation after mid-2015. Strictly
149 gauge-based precipitation estimates were obtained for 1990-2015 from the NOAA
150 Climate Prediction Center's global daily precipitation dataset (28).

151

152 The MODIS active fire detections, precipitation and extinction coefficient from
153 surface visibility were analyzed over the primary burning regions in southern
154 Sumatra (6°S-0°, 99°E-106°E) and south-central Kalimantan (4°S-0, 110°E-117°E).
155 The OMI AI, MODIS AOD, AIRS CO, MOPITT CO and MLS CO were analyzed
156 separately over Sumatra (10°S-10°N, 90°E-105°E) and Kalimantan (10°S-10°N,
157 105°E-120°E) to include the larger regions affected by the smoke. A broader
158 pollution signature is seen in the AIRS, MOPITT and MLS CO, but this will require a
159 more thorough examination of transport mechanisms that was beyond the scope of
160 this study.

3. Results

Figure 2 shows the time-evolution of the 2015 event (black) across the satellite data for Sumatra and Kalimantan, compared with the last major event in 2006 (red). All data have been averaged over the previous 7 days.

In southern Sumatra, the 2015 dry season captured by TRMM precipitation began in mid June, with limited fire activity (< 100 detections / day) appearing late in the month and interrupted by brief periods of rain in mid July and early August. Fire activity increased in late August and by early September, 7-day average fire detections varied around 600 / day. Brief rain during the third week of September caused a temporary decrease in fire activity, which was followed by persistently high fire detections until the return of the monsoon in early November.

The increases in MODIS AOD over the larger region including Sumatra lag the increase in fire activity by roughly 10 days but varied around 0.6 for September, increasing slowly through the first three weeks of October. At the end of October, average AOD increased sharply to ~ 1.4 . The rapid AOD decrease in early November with the arrival of the monsoon lagged by roughly a week behind the drop in fire activity. Increases in OMI AI followed those in the MODIS AOD, but with the timing of peak values (~ 0.9) more closely following the peaks in MODIS fire activity in early and late October. A close examination of the OMI AOD retrieval showed that while pixels with low to moderate loading of aerosols were reported as the 'best' quality data, retrievals with higher reflectivity (> 0.3) at 388nm are flagged as less reliable in the AOD inversion. OMI pixels having reflectivity larger than 0.3 directly over the biomass burning are excluded from the retrieval process due to higher reflectivity that is often associated with the clouds. However, the UV-AI is derived and reported for all-sky conditions regardless of reflectivity of the scene.

The signature of the event can be seen in the MOPITT CO retrieval from the surface to 200 hPa, but is particularly distinct at 500 hPa. CO in the mid-troposphere lags behind the increases in fire activity and aerosols through August and September. MOPITT requires cloud-free observations for CO retrievals so many scenes over Indonesia are excluded. Of the remaining high-quality retrievals, CO approached 300ppbv, slightly higher than in 2006, but the amount of missing data in 2015 makes a comparison between years difficult.

The AIRS CO at 500 hPa had less missing data due to greater data coverage and the use of extrapolation to cloud-free radiances prior to the retrieval. By October, CO increased to concentrations as high as 300 ppbv, dropping sharply in early November with the return of the monsoon. The MLS CO at 215 hPa (~ 12 km in altitude over Sumatra) increased steadily through September, and varied slightly above 200ppbv during the first three weeks of October. A rapid increase to CO exceeding 400 ppbv at the end of October corresponded to the sharp increases in the MODIS AOD. In the uppermost troposphere at 100hPa (~ 16 km), the increase in CO only began in mid October, but rapidly approached 175 ppbv before the end of the burning season.

207

208 Fire activity and pollution for 2006 over Sumatra showed similar precipitation-
209 driven timing to 2015, but was overall lower in magnitude and shorter in duration.
210 MLS CO at 215hPa briefly exceeded 200ppbv and at 100hPa mostly remained below
211 100ppbv. The less severe conditions in 2006 were due to more precipitation from
212 June through mid-September.

213

214 Over Kalimantan, the timing of drying, fire activity and tropospheric pollution
215 during 2015 was very similar to that over Sumatra. Fire activity increased in August,
216 varying about 800 detections/day through September. Precipitation in early
217 October caused a temporary decrease in fire activity, MODIS AOD and OMI AI, but
218 was followed in late October by sharp increases similar to Sumatra, particularly in
219 the aerosol-related retrievals. AIRS and MOPITT CO at 500 hPa varied around 225
220 ppbv for October, with fewer excluded MOPITT profiles than for Sumatra. MLS CO
221 showed an increase in late October, as Sumatra, but to lower CO concentrations,
222 briefly exceeding 300 ppbv at 215 hPa and 150 ppbv at 100 hPa. Compared to 2006,
223 the earlier start of fire activity over Kalimantan in 2015 was offset by an earlier
224 onset of the monsoon. Other than higher CO at 100 hPa, 2015 and 2006 were of
225 comparable magnitude over Kalimantan. Even after the fires stopped with the
226 return of the monsoon, both regions continued to have 100 hPa CO well above
227 “background” (60 ppbv) through November 2015.

228

229 This event represents the largest enhancement in the MLS record of CO at 215 hPa
230 (i.e., since August 2004) (Figure 3). The CO peaks approaching 300 ppbv over
231 western Indonesia form part of a broad signature stretching from the western
232 Indian Ocean to the southwest Pacific Ocean, exceeding the extent, magnitude and
233 duration of the 2006 event. High (200 ppbv) is also measured regularly over eastern
234 South America (boxes Sa11 and Sb11) due to burning in the Arc of Deforestation
235 around the Southeastern Amazon and the Cerrado (savanna) further south, but the
236 upper tropospheric CO signature has a much smaller extent than over Indonesia.

237

238 Figure 4 shows the extinction coefficient (B_{ext}) for 2015 along with 1991 and 1997.
239 1994 was also a severe burning year prior to the EOS period and is discussed in the
240 next section. B_{ext} is computed using visibility from three weather stations in each of
241 southern Sumatra and south-central Kalimantan’s main burning regions over which
242 fire activity and precipitation was averaged in Figure 2. Over Sumatra in 2015, the
243 B_{ext} peaks in mid-September and early and late October correspond closely to those
244 seen in fire activity in Figure 2, reinforcing the usefulness of airport visibility as a
245 severe haze indicator in Indonesia. The 2015 B_{ext} increase is more severe and longer
246 in duration than 2006 but is much lower than the 1991 and 1997 episodes. The
247 magnitude of the 1997 event reflects much lower antecedent rainfall beginning in
248 June. The later 1991 peak in early October compared to 1997 was due to significant
249 rainfall in early September. The late October interruption in haze in 1991 also
250 followed significant precipitation. Overall, B_{ext} data indicates that the 2015 haze in
251 southern Sumatra was less severe than 1991 or 1997, which is easy to explain for
252 1997 given the decreased precipitation that year during the exceptionally strong El

253 Niño. However, it is more difficult to explain for 1991, which was only slightly drier
254 than 2015.

255

256 In Kalimantan, 2015 B_{ext} has two peaks in late September and late October that
257 correspond to those in fire activity. 2015 B_{ext} was also lower than 1997 due to the
258 near-absence of precipitation that year between mid July and early October. The
259 early September onset of 2015 haze was comparable to that in 1991 and its
260 termination earlier, but with weaker isolated precipitation events than in 1991,
261 making it slightly more severe.

262

263 Across the satellite observations, we can conclude with a fair amount of certainty
264 that 2015 was a worse fire year than 2006, because of its earlier start in Sumatra,
265 higher fire activity in September over Kalimantan, and despite an earlier end in
266 Kalimantan. There is greater uncertainty associated with the visibility-based B_{ext}
267 record due to possible changes in observing procedures and more missing records
268 in the early 1990s, but the available data suggest more severe 1990s burning in
269 Sumatra compared to 2015, and in Kalimantan less severe burning in 2015 than in
270 1997 but more than 1991.

271

272 To give a more complete picture of the relationship between annual fire or pollution
273 magnitude and the underlying dry conditions, Figure 5 shows the annual mean dry
274 season (August-November) precipitation plotted against the different fire and haze
275 indicators, for all years over which each source of data are available. Mean
276 precipitation is averaged over the previous 12 weeks to include the effects of
277 antecedent drying for each month during the dry season. In each case, we estimated
278 the strength of the non-linear relationship using piecewise linear regression, which
279 includes an estimated change-point parameter α . We interpret α as the precipitation
280 threshold below which fire and pollution magnitude increase rapidly, and above
281 which, conditions are too wet for high fire activity and pollution. The estimates of α
282 also provide an empirical means of separating severe from non-severe fire years.

283

284 There is a consistently non-linear relationship between dry season precipitation and
285 the different indicators of fire and pollution. Across all indicators of fire and haze
286 during the EOS period, the estimates of α ranged from 3.9 mm/day to 5.2 mm/day.
287 That is, for average dry-season precipitation greater than 6mm/day, there is little
288 fire activity or pollution. Between 4-6 mm/day, there is some increase in fire and
289 pollution, and below 4mm/day, fire and pollution increase rapidly. This has been
290 seen before over broadly the same regions for MODIS fire detections (29) and the
291 MODIS-based Global Fire Emissions Database (12). The non-linearity was also seen
292 between seasonal precipitation in B_{ext} , depending on the period considered for
293 Sumatra and Kalimantan (7).

294

295 During the EOS period, the non-linear relationship with precipitation is strongest
296 (R^2 between 0.85 and 0.98 depending on the region) for MODIS AOD, AIRS and
297 MOPITT CO at 500 hPa, and MODIS fire detections. It is still present, but weaker (R^2
298 between 0.69 and 0.90) for the OMI AI, and MLS CO at both levels, presumably due

299 to their higher-altitude retrieval sensitivity, and therefore additional dependence on
300 a vertical transport mechanism, which has been examined for Indonesian biomass
301 burning using different transport models (30-32). The greatest separation between
302 Sumatra and Kalimantan is for the MLS 215 hPa CO and precipitation relationships.
303 We speculate that at this altitude, pollutant concentrations are strongly dependent
304 on nearby deep convection, but that higher at 100 hPa, there is a greater influence of
305 horizontal advection and the subsequent mixing of pollutants between the two
306 regions. This is supported by a parameterized case study (32) for the 2006 event, in
307 which the convective supply of CO from the surface peaked at 200 hPa, and was very
308 limited at 100 hPa.

309

310 For the longer-term B_{ext} haze proxy, there is a strong non-linear relationship with
311 precipitation over Sumatra ($R^2=0.90$), which weakens over Kalimantan ($R^2=0.77$).
312 This difference is due to a weaker linear relationship over Kalimantan for years with
313 seasonal precipitation below the estimated 3.7mm/day threshold, which is
314 discussed further below.

315

316 **Discussion**

317 Fire activity is known to increase in the tropics during droughts, as long as fuels are
318 abundant (33). But the consistency and non-linearity of this relationship in
319 Indonesia across such a diverse set of satellite-based measurements during the EOS
320 era is remarkable. We are unaware of any other large region where interannual
321 variation in fire activity and pollution through the depth of the troposphere is so
322 strongly, and non-linearly, related to the dry conditions on the ground. The
323 uniqueness of the relationship for Indonesia is due to the ubiquitous use of fire that
324 grows out of control during droughts, its large area of degraded peatlands, and,
325 presumably, the strong control that precipitation has over whether the peat
326 becomes dry enough to burn (34).

327

328 The B_{ext} plot in Figure 5 suggests an increase in fire sensitivity over Kalimantan
329 since the 1990s. Despite occurring under comparably dry, or even wetter
330 conditions, the burning in 2006, 2015, and also 2002, was more severe than in 1991
331 and 1994, which is what weakens the non-linear relationship with precipitation
332 compared to Sumatra. This would represent a continuation of an increase in fire
333 sensitivity over Kalimantan (7). That increase was the result of an absence of severe
334 fire in the 1960s and 1970s despite regularly occurring drought years. Severe fire
335 appeared only in the 1980s, and strengthened in the 1990s, which was attributed to
336 intensifying land use change (7). In southern Sumatra, 2015 and 2006 were
337 somewhat less severe than 1994 despite similar seasonal rainfall, perhaps
338 suggesting a decrease in fire sensitivity. This could correspond to an increase in fire
339 prevention and suppression on larger industrial plantations in the provinces of
340 South Sumatra and Jambi, or to a northward shift in the intensiveness of fire, as
341 noted by recent case studies during the secondary dry season in Riau province (10,
342 12) and satellite records of tree-cover loss (35). Possible changes in fire sensitivity
343 inferred from B_{ext} will need to be studied further, taking into account changes in
344 data completeness, the effect of different year-to-year transport patterns relative to

345 the airport locations, and most importantly, corroboration with estimates of
346 changing land use.

347
348 Since 1997, annual emissions from fires in all of Indonesia have been between 6 (in
349 2010) and 1046 (in 1997) Tg C according to the Global Fire Emissions Database
350 version 4s (GFED4s), updated from previous versions (36). Total emissions for 2015
351 were estimated to be 380 Tg C, which translates to 1.5 billion metric tons CO₂
352 equivalent when also including emissions of methane and nitrous oxide. This is in
353 between the 2013 annual fossil fuel CO₂ emissions of Japan and India (37). Known
354 sources of uncertainty in the emissions estimate are a possible underestimation of
355 burned area due to cloud and smoke cover (38) and a possible overestimation
356 relating to recent work (39, 40) showing that the depth of peat burning decreases
357 for successive fires, which is not yet taken account for repeated fires in the same
358 area in GFED4s. Viewed historically, these events are nevertheless a large part of
359 what makes Indonesia's land use change-related greenhouse gas emissions much
360 larger than its fossil fuel emissions when compared to other countries (41).

361
362 Eliminating fire from degraded peatlands is a long-term goal and will require major
363 reforms in land use and land tenure in the context of Indonesia's need for economic
364 development. In the short term, fire prevention, suppression and mitigation
365 measures must be tied to early warning triggers. Our analysis over five different
366 indicators of fire activity and atmospheric pollution from NASA EOS data suggests
367 that doing so is a matter of being able to anticipate extended periods of less than
368 4mm/day of rain. Given the skill with which strong El Niño impacts can increasingly
369 be predicted (42, 43) tying these predictions to early warning triggers based on
370 these types of precipitation thresholds should be a priority.

371 372 **Acknowledgements**

373 The MODIS, MOPITT, AIRS, MLS and OMI projects are supported by the NASA Earth
374 Observing System Program. The National Center for Atmospheric Research is
375 sponsored by the National Science Foundation. RF was supported by the NASA
376 Atmospheric Chemistry Modeling and Analysis Program and the NASA Precipitation
377 Measurement Missions Science Team, and GvdW and TF by the European Research
378 Council. Part of the research was carried out at the Jet Propulsion Laboratory,
379 California Institute of Technology, under a contract with the National Aeronautics
380 and Space Administration. Resources supporting this work were provided by the
381 NASA High-End Computing Program through the NASA Center for Climate
382 Simulation at Goddard Space Flight Center. AIRS CO, MODIS AOD and TRMM
383 precipitation data were obtained from the NASA GIOVANNI system. All data in the
384 study can be obtained by contacting the lead author

References

1. Voiland A (2015) Seeing Through the Smoky Pall: Observations from a Grim Indonesian Fire Season. (NASA Earth Observatory).
2. Malingreau JP, Stephens G, & Fellows L (1985) Remote-sensing of forest fires - Kalimantan and North Borneo in 1982-83. *Ambio* 14(6):314-321.
3. Fishman J, Watson CE, Larsen JC, & Logan JA (1990) Distribution of tropospheric ozone determined from satellite data. *Journal of Geophysical Research-Atmospheres* 95(D4):3599-3617.
4. Kita K, Fujiwara M, & Kawakami S (2000) Total ozone increase associated with forest fires over the Indonesian region and its relation to the El Nino-Southern oscillation. *Atmospheric Environment* 34(17):2681-2690.
5. Thompson AM, *et al.* (2001) Tropical tropospheric ozone and biomass burning. *Science* 291(5511):2128-2132.
6. Wooster MJ, Perry GLW, & Zoumas A (2012) Fire, drought and El Nino relationships on Borneo (Southeast Asia) in the pre-MODIS era (1980-2000). *Biogeosciences* 9(1):317-340.
7. Field RD, van der Werf GR, & Shen SSP (2009) Human amplification of drought-induced biomass burning in Indonesia since 1960. *Nature Geoscience* 2(3):185-188.
8. Herawati H & Santoso H (2011) Tropical forest susceptibility to and risk of fire under changing climate: A review of fire nature, policy and institutions in Indonesia. *Forest Policy and Economics* 13(4):227-233.
9. Medrilzam M, Dargusch P, Herbohn J, & Smith C (2014) The socio-ecological drivers of forest degradation in part of the tropical peatlands of Central Kalimantan, Indonesia. *Forestry* 87(2):335-345.
10. Gaveau DLA, *et al.* (2014) Major atmospheric emissions from peat fires in Southeast Asia during non-drought years: evidence from the 2013 Sumatran fires. *Scientific Reports* 4.
11. Page SE, *et al.* (2002) The amount of carbon released from peat and forest fires in Indonesia during 1997. *Nature* 420(6911):61-65.
12. Field RD & Shen SSP (2008) Predictability of carbon emissions from biomass burning in Indonesia from 1997 to 2006. *Journal of Geophysical Research-Biogeosciences* 113(G4):17.
13. Logan JA, *et al.* (2008) Effects of the 2006 El Nino on tropospheric composition as revealed by data from the Tropospheric Emission Spectrometer (TES). *Geophysical Research Letters* 35(3):5.
14. Yurganov L, McMillan W, Grechko E, & Dzhola A (2010) Analysis of global and regional CO burdens measured from space between 2000 and 2009 and validated by ground-based solar tracking spectrometers. *Atmospheric Chemistry and Physics* 10(8):3479-3494.
15. Worden J, *et al.* (2013) El Nino, the 2006 Indonesian peat fires, and the distribution of atmospheric methane. *Geophysical Research Letters* 40(18):4938-4943.
16. Livesey NJ, *et al.* (2013) Interrelated variations of O-3, CO and deep convection in the tropical/subtropical upper troposphere observed by the

- Aura Microwave Limb Sounder (MLS) during 2004-2011. *Atmospheric Chemistry and Physics* 13(2):579-598.
17. Deeter MN, *et al.* (2013) Validation of MOPITT Version 5 thermal-infrared, near-infrared, and multispectral carbon monoxide profile retrievals for 2000-2011. *Journal of Geophysical Research-Atmospheres* 118(12):6710-6725.
 18. Warner J, Carminati F, Wei Z, Lahoz W, & Attie JL (2013) Tropospheric carbon monoxide variability from AIRS under clear and cloudy conditions. *Atmospheric Chemistry and Physics* 13(24):12469-12479.
 19. Livesey NJ, *et al.* (2015) Earth Observing System Aura Microwave Limb Sounder Version 4.2x Level 2 data quality and description document. (Jet Propulsion Laboratory / California Institute of Technology, Pasadena, CA), p 162.
 20. Remer LA, *et al.* (2008) Global aerosol climatology from the MODIS satellite sensors. *Journal of Geophysical Research-Atmospheres* 113(D14).
 21. Levy RC, Remer LA, Mattoo S, Vermote EF, & Kaufman YJ (2007) Second-generation operational algorithm: Retrieval of aerosol properties over land from inversion of Moderate Resolution Imaging Spectroradiometer spectral reflectance. *Journal of Geophysical Research-Atmospheres* 112(D13).
 22. Torres O, Ahn C, & Chen Z (2013) Improvements to the OMI near-UV aerosol algorithm using A-train CALIOP and AIRS observations. *Atmospheric Measurement Techniques* 6(11):3257-3270.
 23. Giglio L, Descloitres J, Justice CO, & Kaufman YJ (2003) An enhanced contextual fire detection algorithm for MODIS. *Remote Sensing of Environment* 87(2-3):273-282.
 24. Heil A & Goldammer JG (2001) Smoke-haze pollution: a review of the 1997 episode in Southeast Asia. *Regional Environmental Change* 2(1):24-37.
 25. Wang YH, Field RD, & Roswintiarti O (2004) Trends in atmospheric haze induced by peat fires in Sumatra Island, Indonesia and El Nino phenomenon from 1973 to 2003. *Geophysical Research Letters* 31(4).
 26. Field RD, Wang Y, Roswintiarti O, & Guswanto (2004) A drought-based predictor of recent haze events in western Indonesia. *Atmospheric Environment* 38(13):1869-1878.
 27. Huffman GJ, *et al.* (2007) The TRMM multisatellite precipitation analysis (TMPA): Quasi-global, multiyear, combined-sensor precipitation estimates at fine scales. *Journal of Hydrometeorology* 8(1):38-55.
 28. Chen MY, *et al.* (2008) Assessing objective techniques for gauge-based analyses of global daily precipitation. *Journal of Geophysical Research-Atmospheres* 113(D4):13.
 29. van der Werf GR, *et al.* (2008) Climate regulation of fire emissions and deforestation in equatorial Asia. *Proceedings of the National Academy of Sciences of the United States of America* 105(51):20350-20355.
 30. Nassar R, *et al.* (2009) Analysis of tropical tropospheric ozone, carbon monoxide, and water vapor during the 2006 El Nino using TES observations and the GEOS-Chem model. *Journal of Geophysical Research-Atmospheres* 114:23.

31. Ott L, Pawson S, & Bacmeister J (2011) An analysis of the impact of convective parameter sensitivity on simulated global atmospheric CO distributions. *Journal of Geophysical Research-Atmospheres* 116.
32. Field RD, *et al.* (2015) Sensitivity of simulated tropospheric CO to subgrid physics parameterization: a case study of Indonesian biomass burning emissions in 2006. *Journal of Geophysical Research - Atmospheres* 120.
33. van der Werf GR, Randerson JT, Giglio L, Gobron N, & Dolman AJ (2008) Climate controls on the variability of fires in the tropics and subtropics. *Global Biogeochemical Cycles* 22(3).
34. Rein G, Cleaver N, Ashton C, Pironi P, & Torero JL (2008) The severity of smouldering peat fires and damage to the forest soil. *Catena* 74(3):304-309.
35. Hansen MC, *et al.* (2013) High-Resolution Global Maps of 21st-Century Forest Cover Change. *Science* 342(6160):850-853.
36. van der Werf GR, *et al.* (2010) Global fire emissions and the contribution of deforestation, savanna, forest, agricultural, and peat fires (1997-2009). *Atmospheric Chemistry and Physics* 10(23):11707-11735.
37. Janssens-Maenhout G, *et al.* (2012) EDGAR-HTAP: a Harmonized Gridded Air Pollution Emission Dataset Based on National Inventories. (European Commission Publications Office, Ispra, Italy).
38. Giglio L, Randerson JT, & van der Werf GR (2013) Analysis of daily, monthly, and annual burned area using the fourth-generation global fire emissions database (GFED4). *Journal of Geophysical Research-Biogeosciences* 118(1):317-328.
39. Ballhorn U, Siegert F, Mason M, & Limin S (2009) Derivation of burn scar depths and estimation of carbon emissions with LIDAR in Indonesian peatlands. *Proceedings of the National Academy of Sciences of the United States of America* 106(50):21213-21218.
40. Konecny K, *et al.* (2016) Variable carbon losses from recurrent fires in drained tropical peatlands. *Global Change Biology* 22(4):1469-1480.
41. WRI (2015) CAIT Climate Data Explorer. (World Resources Institute, Washington, DC).
42. Li S & Robertson AW (2015) Evaluation of Submonthly Precipitation Forecast Skill from Global Ensemble Prediction Systems. *Monthly Weather Review* 143(7):2871-2889.
43. Spessa AC, *et al.* (2015) Seasonal forecasting of fire over Kalimantan, Indonesia. *Natural Hazards and Earth System Sciences* 15(3):429-442.

List of figures

- Figure 1. 2015 high confidence Aqua and Terra MODIS active fire density (Ref 23)($0.25^\circ \times 0.25^\circ$) over Sumatra and Borneo for a) August, b) September, c) October and d) November.
- Figure 2. Time series of various species for 2015 and 2006 over Sumatra and Kalimantan. OMI AI, MODIS AOD, MOPITT CO, AIRS CO and MLS CO are averaged for Sumatra over ($10^\circ\text{S}-10^\circ\text{N}$, $90^\circ\text{E}-105^\circ\text{E}$) and for Kalimantan over ($10^\circ\text{S}-10^\circ\text{N}$, $105^\circ\text{E}-120^\circ\text{E}$). MODIS active fires and TRMM precipitation are averaged over the smaller primary burning regions, for Sumatra ($6^\circ\text{S}-0^\circ$, $99^\circ\text{E}-106^\circ\text{E}$) and for Kalimantan ($4^\circ\text{S}-0^\circ$, $110^\circ\text{E}-117^\circ\text{E}$). Subscripts for the MLS, AIRS and MOPITT CO are the altitude in hPa over which the data were analyzed. All data have been averaged over the previous 7 days.
- Figure 3. Bi-weekly averaged MLS CO at 215 hPa ($\sim 12\text{km}$) for $15^\circ \times 30^\circ$ cells during 2004-2015. Line colors denote year. Numbers and letters in black boxes along the top and right edges identify regions for discussion in the text.
- Figure 4. NOAA Climate Prediction Center (CPC) gauged-based precipitation and extinction coefficient (B_{ext}) calculated from horizontal visibility. CPC precipitation averaged over the smaller primary burning regions, for Sumatra ($6^\circ\text{S}-0^\circ$, $99^\circ\text{E}-106^\circ\text{E}$) and for Kalimantan ($4^\circ\text{S}-0^\circ$, $110^\circ\text{E}-117^\circ\text{E}$) for three high fire years. Extinction coefficient calculated over Sumatra from the airports in Rengat, Jambi and Palembang, and over Kalimantan from Pangkalan Bun, Palangkaraya and Muaratewe. All data have been averaged over the previous 7 days.
- Figure 5. Annual August-November relationships between CPC precipitation over the source regions and fire/pollution metrics. Subscripts for the MLS, AIRS and MOPITT CO are the altitude in hPa over which the data were analyzed. The numbers above each point are the last two digits of each year. Dashed lines show the piecewise-linear regression fit for each region, the coefficient of determination (R^2) and change-point estimate (α) for which are provided in the figure legends.

Figures

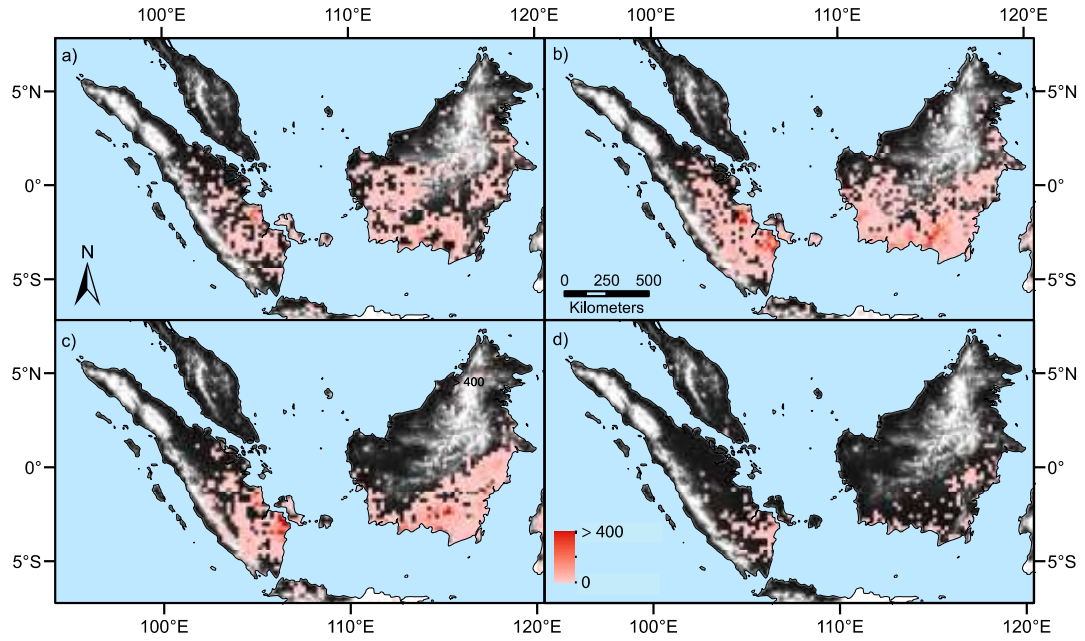


Figure 1. 2015 high confidence Aqua and Terra MODIS active fire density ($0.25^\circ \times 0.25^\circ$) over Sumatra and Borneo for a) August, b) September, c) October and d) November.

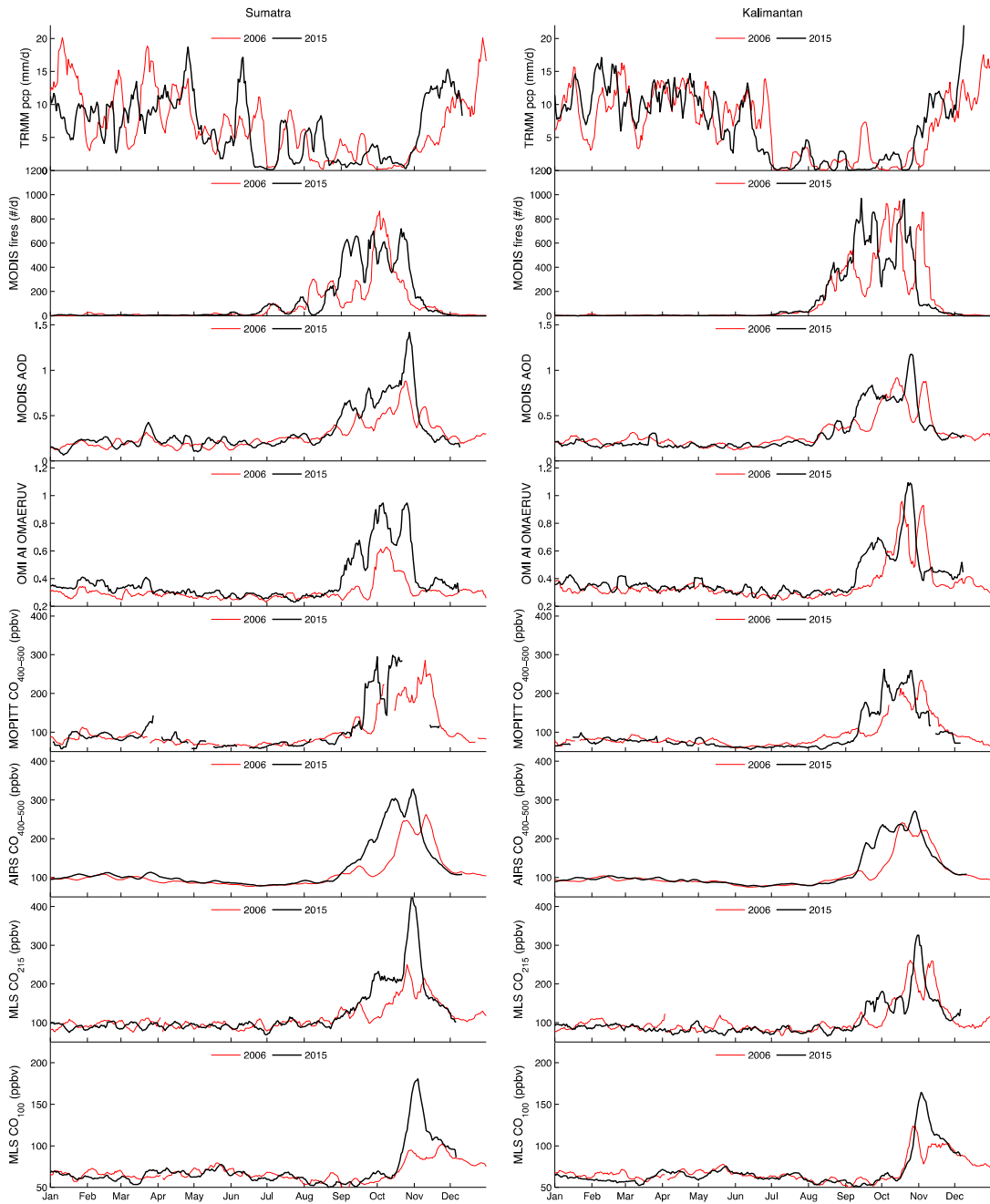


Figure 2. Time series of various species for 2015 and 2006 over Sumatra and Kalimantan. OMI AI, MODIS AOD, MOPITT CO, AIRS CO and MLS CO are averaged for Sumatra over (10S-10N, 90E-105E) and for Kalimantan over (10S-10N, 105E-120E). MODIS active fires and TRMM precipitation are averaged over the smaller primary burning regions, for Sumatra (6S-0, 99E-106E) and for Kalimantan (4S-0, 110E-117E). Subscripts for the MLS, AIRS and MOPITT CO are the altitude in hPa over which the data were analyzed. All data have been averaged over the previous 7 days.

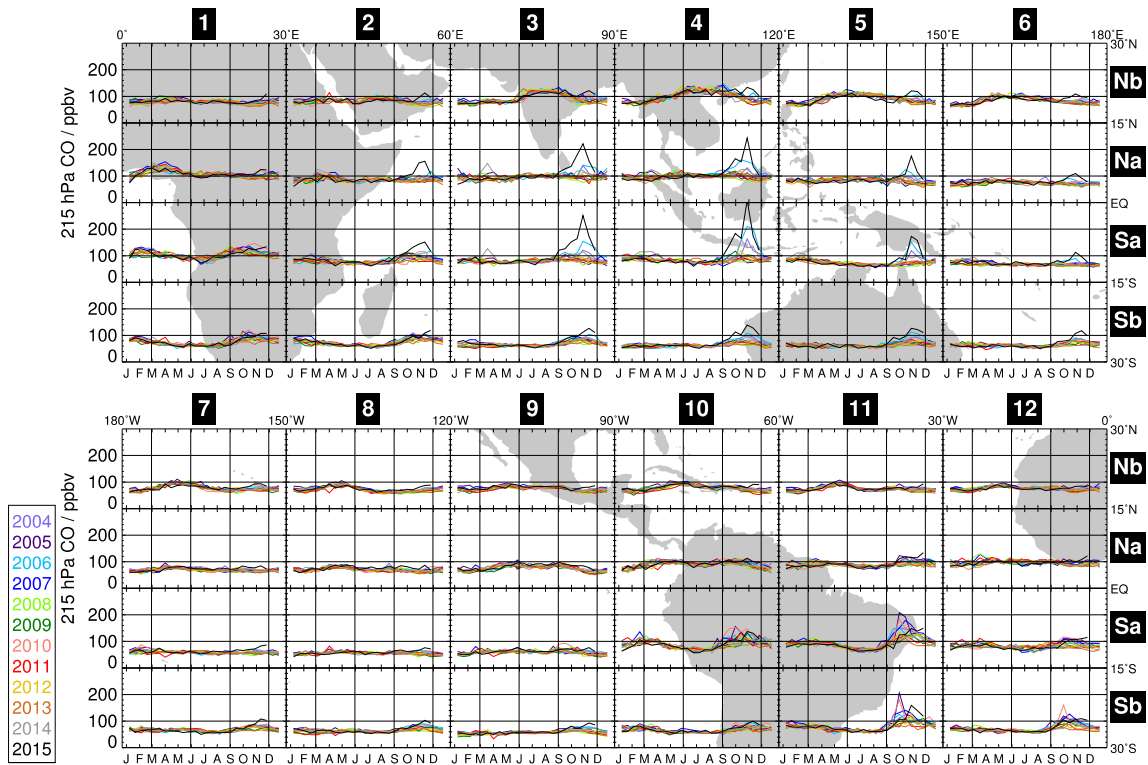


Figure 3. Bi-weekly averaged MLS CO at 215 hPa (~12km) for 15° x 30° cells during 2004-2015. Line colors denote year. Numbers and letters in black boxes along the top and right edges identify regions for discussion in the text.

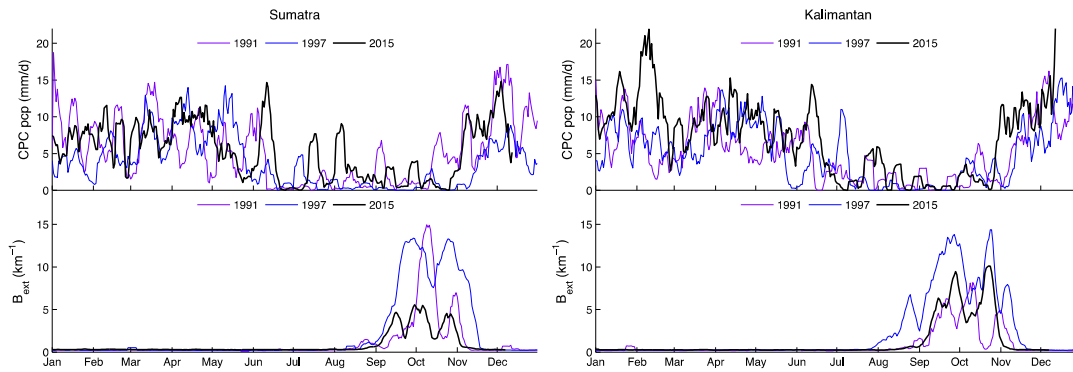


Figure 4. NOAA Climate Prediction Center (CPC) gauged-based precipitation and extinction coefficient (B_{ext}) calculated from horizontal visibility. CPC precipitation averaged over the smaller primary burning regions, for Sumatra (6S-0, 99E-106E) and for Kalimantan (4S-0, 110E-117E) for three high fire years. Extinction coefficient calculated over Sumatra from the airports in Rengat, Jambi and Palembang, and over Kalimantan from Pangkalan Bun, Palangkaraya and Muaratewe. All data have been averaged over the previous 7 days.

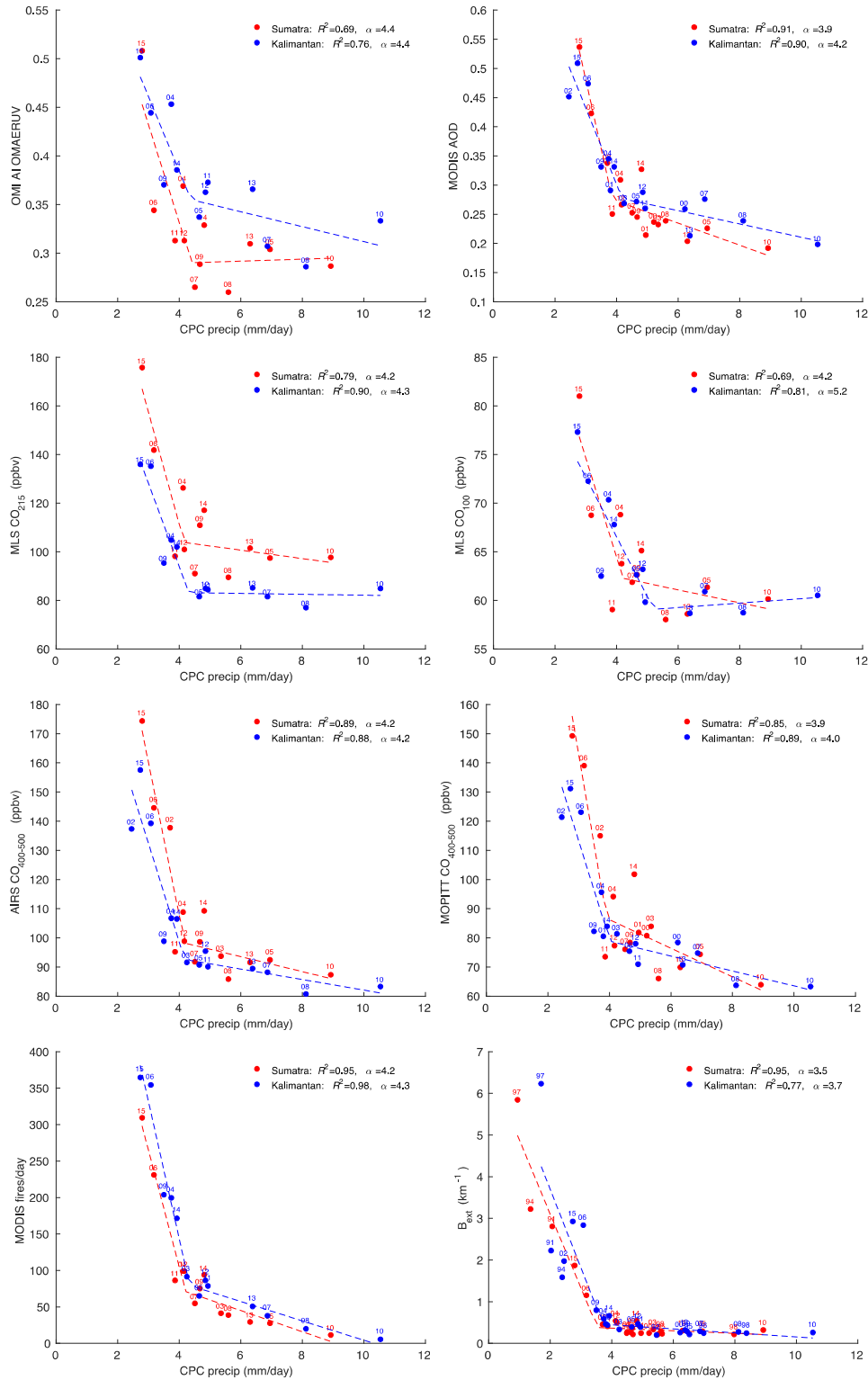


Figure 5. Annual August-November relationships between CPC precipitation over the source regions and fire/pollution metrics. Subscripts for the MLS, AIRS and MOPITT CO are the altitude in hPa over which the data were analyzed. The numbers above each point are the last two digits of each year. Dashed lines show the piecewise-linear regression fit for each region, the coefficient of determination (R^2) and change-point estimate of precipitation (α , mm/day) for which are provided in the figure legends.